Multiple chiral doublets in four-j shells particle rotor model: Five possible chiral doublets in $^{136}_{60}\text{Nd}_{76}$

Q.B. Chen [a], B.F. Lv [b], C.M. Petrache [b], J. Meng [c,d,e,*]

[a] *Physik-Department, Technische Universität München, D-85747 Garching, Germany*
[b] *Centre de Sciences Nucléaires et Sciences de la Matière, CNRS/IN2P3, Université Paris-Saclay, Bât. 104-108, 91405 Orsay, France*
[c] *State Key Laboratory of Nuclear Physics and Technology, School of Physics, Peking University, Beijing 100871, China*
[d] *Yukawa Institute for Theoretical Physics, Kyoto University, Kyoto 606-8502, Japan*
[e] *Department of Physics, University of Stellenbosch, Stellenbosch, South Africa*

A B S T R A C T

A particle rotor model, which couples nucleons in four single-j shells to a triaxial rotor core, is developed to investigate the five pairs of nearly degenerate doublet bands recently reported in the even-even nucleus ^{136}Nd. The experimental energy spectra and available $B(M1)/B(E2)$ values are successfully reproduced. The angular momentum geometries of the valence nucleons and the core support the chiral rotation interpretations not only for the previously reported chiral doublet, but also for the other four candidates. Hence, ^{136}Nd is the first even-even candidate nucleus in which the multiple chiral doublets exist. Five pairs of chiral doublet bands in a single nucleus is also a new record in the study of nuclear chirality.

Chiral rotation is an exotic rotational mode in a nucleus with triaxial ellipsoidal shape. The rotations about an axis out of the three principal planes of the triaxial nucleus can give rise to a pair of near degenerate $\Delta I = 1$ bands with the same parity, i.e., chiral doublet bands [1]. Chiral rotation was well established in the $A \sim$ 80, 100, 130, and 190 mass regions in odd–odd nuclei [2–7] and odd-A nuclei [8–10]. For details, see recent reviews [11–17] or data tables [18].

However, chiral doublet bands were rarely observed in even-even nuclei. The general opinion for this is that the multi-quasiparticle configurations become more complex and involve at least two valence protons and two valence neutrons. In Ref. [19], two doublet bands were observed in the even-even isotopes ^{110,112}Ru and interpreted as soft chiral vibrations.

Very recently, five pairs of nearly degenerate doublet bands were reported in the even-even nucleus ^{136}Nd, which were discovered in a high-statistics experiment performed with the high-efficiency Jurogam II array [20]. It was demonstrated that the chiral partners of strongly populated bands in the triaxial nucleus are present close to yrast, as in the case of the odd–odd and odd–even nuclei, but are far weaker than the yrast partners and therefore not easy to observe. The observed five pairs of nearly degenerate

bands were investigated by the constrained and tilted axis cranking covariant density functional theory (TAC-CDFT) [21–25]: one of them is revealed to be a chiral doublet, and the other four are chiral candidates [20]. These observations shed new light on the investigations of chiral doublets in even-even nuclei. If the four chiral candidates are finally confirmed, then they will constitute a multiple chiral doublet (MχD), a phenomenon predicted by covariant density functional theory (CDFT) [21,26–29] and particle rotor model (PRM) [30–33], and observed experimentally [34–36]. The future identification of such bands in ^{136}Nd will hopefully open a campaign of measurements for other even-even triaxial nuclei, in which the chirality or the MχD phenomenon could exist.

Theoretically, various approaches have been developed extensively to investigate the chiral doublet bands. For example, the PRM [1,37–41], the TAC approach [24,42–44], the TAC plus random-phase approximation (RPA) [45], the collective Hamiltonian method [46,47], the interacting boson model [48,49], and the angular momentum projection (AMP) [50–53]. In addition, the generalized coherent state model (GCSM) was also applied to triaxial even-even nuclei and a different formalism of chiral rotation was proposed [54–57].

In Ref. [20], as mentioned above, the observed doublet bands in ^{136}Nd were investigated in the framework of the TAC-CDFT [22–25], which is a fully microscopic approach, but cannot describe the energy splitting and the quantum tunneling between the chi-

Table 1

The parities, unpaired nucleon configurations, quadrupole deformation parameters (β, γ), moments of inertia $\mathcal{J}_0$ (unit $\hbar^2/\text{MeV}$), and Coriolis attenuation factors ξ used in the PRM calculations for bands D1–D6 and their partners.

Band	Parity	Unpaired nucleons	(β, γ)	$\mathcal{J}_0$	ξ
D1	+	$\pi(1h_{11/2})^1(2d_{5/2})^{-1} \otimes \nu(1h_{11/2})^{-1}(2d_{3/2})^{-1}$	$(0.21, 21°)$	32.0	0.96
D2	+	$\pi(1h_{11/2})^3(2d_{5/2})^{-1} \otimes \nu(1h_{11/2})^{-1}(2d_{3/2})^{-1}$	$(0.22, 19°)$	35.0	0.96
D5	+	$\pi(1h_{11/2})^2(1g_{7/2})^{-2} \otimes \nu(1h_{11/2})^{-1}(1f_{7/2})^1$	$(0.26, 23°)$	40.0	0.93
D3	−	$\pi(1h_{11/2})^2 \otimes \nu(h_{11/2})^{-1}(2d_{3/2})^{-1}$	$(0.22, 19°)$	32.0	0.97
D4	−	$\pi(1h_{11/2})^2(2d_{5/2})^{-2} \otimes \nu(h_{11/2})^{-1}(2d_{3/2})^{-1}$	$(0.22, 19°)$	33.0	0.97
D6	−	$\pi(1h_{11/2})^3(2d_{5/2})^{-1} \otimes \nu(h_{11/2})^{-1}(1f_{7/2})^1$	$(0.23, 25°)$	42.0	0.95

ral doublet bands. The aim of the present work is to investigate the chirality of ^{136}Nd in the framework of PRM. PRM is a quantal model coupling the collective rotation and the single-particle motions. In contrast to the TAC approach, it describes a system in the laboratory frame. The total Hamiltonian is diagonalized with total angular momentum as a good quantum number, and the energy splitting and quantum tunneling between the doublet bands can be obtained directly. Moreover, the basic microscopic inputs for PRM can be obtained from the constrained CDFT [10,21,25,34–36, 58].

Various versions of PRM have been developed to investigate the chiral doublet bands with different kinds of configurations. For example, the PRM with one-particle-one-hole configuration was used to describe the chirality in odd–odd nuclei [1,33,37,38,59]. To simulate the effects of many valence nucleons, pairing correlations were introduced and PRM with two quasiparticles configuration was developed [39,60–65]. To describe the odd-A nuclei, the many-particle-many-hole versions of PRM with nucleons in two single-j shells [40,66] or three single-j shells [34,35,58,67], have been developed. It is noted that the unpaired nucleon configurations of the doublet bands in the even-even nucleus ^{136}Nd involve four different single-j shells. Such PRM is still unavailable.

In this letter, a PRM that couples nucleons in four single-j shells to a triaxial rotor core is developed and applied to study the energy spectra, the electromagnetic transition probabilities, as well as the angular momentum geometries for the observed doublet bands in ^{136}Nd.

The formalism of the PRM in the present work is an extension of that in Ref. [40], where the many-particle-many-hole version of PRM with two single-j shells was developed. The total Hamiltonian of PRM is expressed as

$$\hat{H}_{\text{PRM}} = \hat{H}_{\text{coll}} + \hat{H}_{\text{intr}}, \tag{1}$$

with the collective rotor Hamiltonian

$$\hat{H}_{\text{coll}} = \sum_{k=1}^{3} \frac{\hat{R}_k^2}{2\mathcal{J}_k} = \sum_{k=1}^{3} \frac{(\hat{I}_k - \hat{J}_k)^2}{2\mathcal{J}_k}, \tag{2}$$

where the indexes $k = 1$, 2, and 3 refer to the three principal axes of the body-fixed frame. The $\hat{R}_k$ and $\hat{I}_k$ denote the angular momentum operators of the core and of the total nucleus, respectively, and the $\hat{J}_k$ is the total angular momentum operator of the valence nucleons. The moments of inertia of the irrotational flow type [68] are adopted, i.e., $\mathcal{J}_k = \mathcal{J}_0 \sin^2(\gamma - 2k\pi/3)$, with γ the triaxial deformation parameter. In addition, the intrinsic Hamiltonian is written as

$$H_{\text{intr}} = \sum_{i=1}^{4} \sum_{\nu} \varepsilon_{i,\nu} a_{i,\nu}^\dagger a_{i,\nu}, \tag{3}$$

where $\varepsilon_{i,\nu}$ is the single particle energy in the i-th single-j shell provided by

$$h_{\text{sp}} = \pm\frac{1}{2}C\left\{\cos\gamma\left(j_3^2 - \frac{j(j+1)}{3}\right) + \frac{\sin\gamma}{2\sqrt{3}}\left(j_+^2 + j_-^2\right)\right\}. \tag{4}$$

Here, the plus or minus sign refers to particle or hole, and the coefficient C is proportional to the quadrupole deformation β as in Ref. [69].

The single particle state and its time reversal state are expressed as

$$a_\nu^\dagger|0\rangle = \sum_{\alpha\Omega} c_{\alpha\Omega}^\nu |\alpha, j\Omega\rangle, \tag{5}$$

$$a_{\bar{\nu}}^\dagger|0\rangle = \sum_{\alpha\Omega} (-1)^{j-\Omega} c_{\alpha\Omega}^\nu |\alpha, j-\Omega\rangle, \tag{6}$$

where Ω is the projection of the single-particle angular momentum j along the 3-axis of the intrinsic frame and restricted to $\dots, -3/2, 1/2, 5/2, \dots$ due to the time-reversal degeneracy, and α denotes the other quantum numbers. For a system with $\sum_{i=1}^{4} N_i$ valence nucleons (N_i denotes the number of the nucleons in the i-th single-j shell), the intrinsic wave function is given as

$$|\varphi\rangle = \prod_{i=1}^{4}\left(\prod_{l=1}^{n_i} a_{i,\nu_l}^\dagger\right)\left(\prod_{l=1}^{n_i'} a_{i,\bar{\mu}_l}^\dagger\right)|0\rangle, \tag{7}$$

with $n_i + n_i' = N_i$ and $0 \le n_i \le N_i$.

The total wave function can be expanded into the strong coupling basis

$$|IM\rangle = \sum_{K\varphi} c_{K\varphi}|IMK\varphi\rangle, \tag{8}$$

with

$$|IMK\varphi\rangle = \frac{1}{\sqrt{2(1+\delta_{K0}\delta_{\varphi,\bar{\varphi}})}}\left(|IMK\rangle|\varphi\rangle + (-1)^{I-K}|IM-K\rangle|\bar{\varphi}\rangle\right), \tag{9}$$

where $|IMK\rangle$ is the Wigner function $\sqrt{\frac{2I+1}{8\pi^2}}D_{MK}^I$. The basis states are symmetrized under the point group D$_2$, which leads to $K - \frac{1}{2}\sum_{i=1}^{4}(n_i - n_i')$ being an even integer.

It is noted that due to the inclusion of many-particle-many-hole configurations with four single-j shells, the size of the basis space is rather large. For example, for the calculations of band D1 in ^{136}Nd (see its configuration in Table 1), the dimension of the basis space is $864(2I+1)$. For $I = 10\hbar$, this value is 18144, and for $I = 20\hbar$, it is 35424. It is quite time-consuming in the diagonalization of the PRM Hamiltonian matrix. To solve this problem, similar in the shell-model-like approach (SLAP) [70,71], we adopt a properly truncated basis space by introducing a cutoff for the configuration energy $\sum_{i,\nu} \varepsilon_{i,\nu}$. In such a way, the dimension of the PRM matrix is reduced to ~ 5000–10000 with the energy uncertainty within 0.1%.
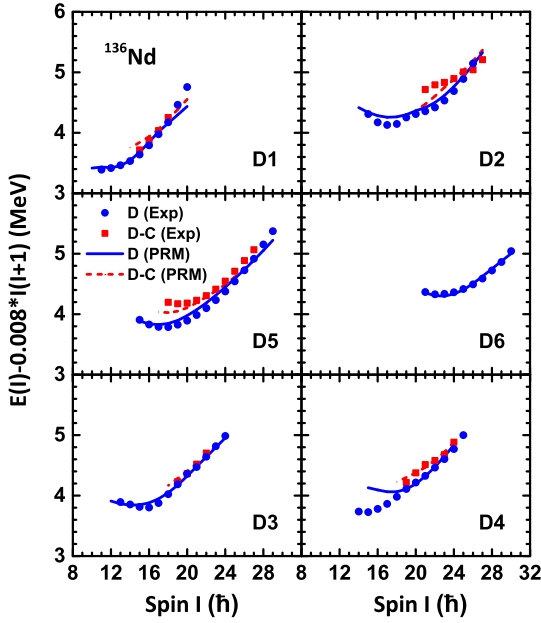
Fig. 1. (Color online.) The energy spectra of bands D1–D6 and their partners calculated by PRM in comparison with corresponding data. The excitation energies are relative to a rigid-rotor reference.

Fig. 2. (Color online.) The staggering parameters of bands D1–D6 calculated by PRM in comparison with corresponding data.

After obtaining the wave functions of PRM, the reduced transition probabilities $B(M1)$ and $B(E2)$, and expectation values of the angular momentum of the system can be calculated.

There are five pairs of doublet bands in ^{136}Nd (labeled as bands D1–D5), in which three of them (bands D1, D2, and D5) have positive parity. Besides, there is a dipole band (labeled as band D6), which has no partner band. In the PRM calculations for these bands, the unpaired nucleon configurations are consistent with those in Ref. [20] and the corresponding quadrupole deformation parameters (β, γ) are obtained from triaxial constrained CDFT calculations [21]. The moments of inertia $\mathcal{J}_0$ and Coriolis attenuation factors ξ are adjusted to reproduce the trend of the energy spectra. The corresponding details are listed in Table 1. In addition, for the electromagnetic transitions, the empirical intrinsic quadrupole moment $Q_0 = (3/\sqrt{5\pi})R_0^2 Z\beta$, and gyromagnetic ratios for rotor $g_R = Z/A$ and for nucleons $g_{p(n)} = g_l + (g_s - g_l)/(2l+1)$ ($g_l = 1(0)$ for protons (neutrons) and $g_s = 0.6g_s$(free)) [68] are adopted.

The calculated energy spectra for the bands D1–D6 in ^{136}Nd are presented in Fig. 1, together with the corresponding data. The experimental energy spectra are reproduced excellently by the PRM calculations. Being a quantum model, PRM is able to reproduce the energy splitting for the whole observed spin region. It is seen that excepting band D2, the trend and amplitude for the energy splitting between partner bands are reproduced well.

For D2 and D5, the energy differences between the doublet bands decrease gradually with the spin. In detail, for D2, the energy splitting is ~ 360 keV at $I = 21\hbar$, and finally goes to ~ 110 keV at $I = 25\hbar$. The PRM calculations underestimate this energy separation. For bands D5 and D5-C, which are identified as chiral doublets in Ref. [20], their energy splitting is ~ 410 keV at $I = 18\hbar$, and reduces to ~ 150 keV at $I = 27\hbar$.

For the other three pairs of doublet bands (D1,D1-C), (D3,D3-C), and (D4,D4-C), the energy separations are about 70, 40, and 120 keV, respectively, and do not change much with the spin. For band D4, the PRM calculations can not reproduce the data below $I = 18\hbar$, indicating that the used configuration is not suitable for the lower spin part. Nevertheless, the rather small energy
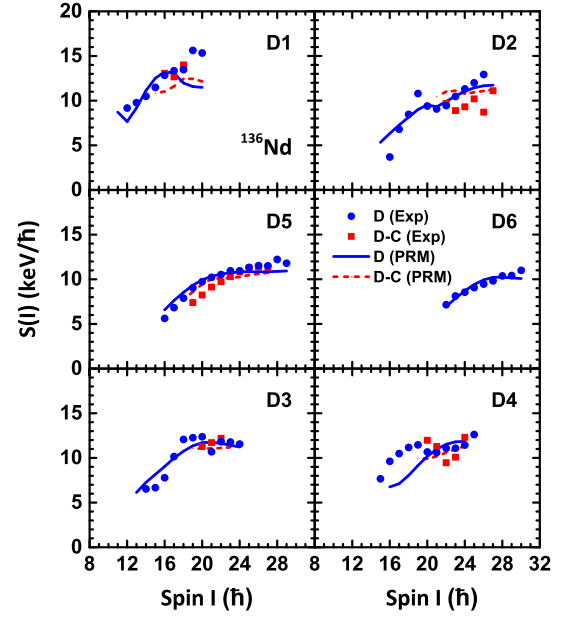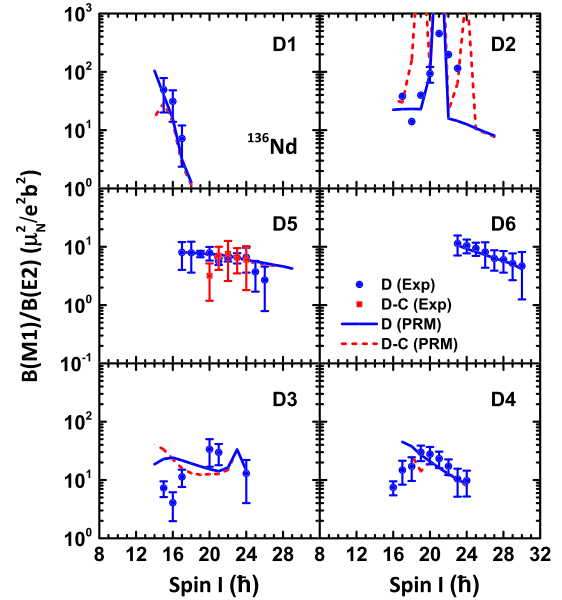

Fig. 3. (Color online.) The $B(M1)/B(E2)$ of bands D1–D6 and their partners calculated by PRM in comparison with corresponding data.

differences between these doublets support that their chiral interpretation.

From the energy spectra, the staggering parameters $S(I) = [E(I) - E(I-1)]/2I$ are extracted and displayed in Fig. 2. The standard fingerprints for chiral bands outlined in Ref. [3] require that $S(I)$ is independent of spin. Overall, the PRM calculations can reproduce the behaviors of experimental $S(I)$. Moreover, the $S(I)$ of all bands vary smoothly and do not change much with spin. These phenomena further provide the support that the bands D1–D5 are chiral partners.

In Fig. 3, the $B(M1)/B(E2)$ values of bands D1–D6 calculated by PRM in comparison with the corresponding experimental data are shown. One observes that the PRM calculations show an impressive agreement with the data. Moreover, excepting band D2
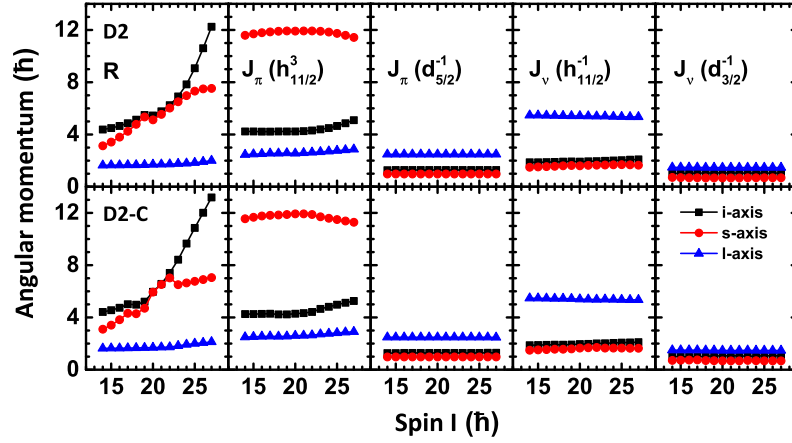
Fig. 4. (Color online.) The root mean square components along the intermediate (i-, squares), short (s-, circles) and long (l-, triangles) axes of the rotor, valence protons, and valence neutrons angular momenta calculated as functions of spin by PRM for the doublet bands D2 and D2-C in ^{136}Nd.
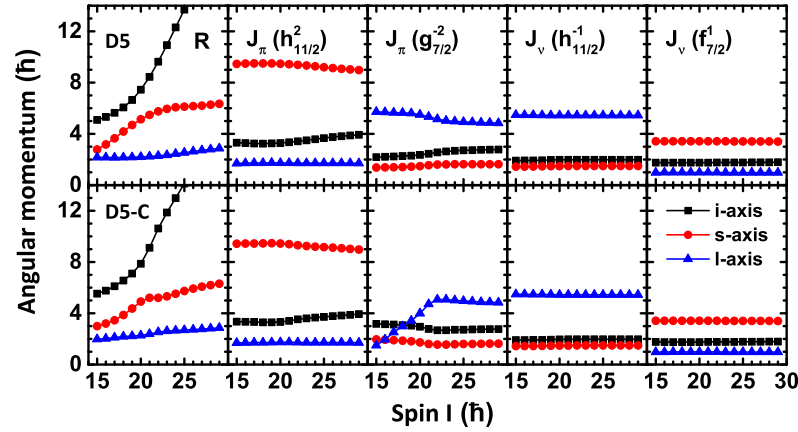

Fig. 5. (Color online.) Same as Fig. 4, but for D5.

the calculated $B(M1)/B(E2)$ values of the doublet bands are rather similar.

For bands D1 and D6, the $B(M1)/B(E2)$ values decrease with spin. For D2, an abrupt increase of $B(M1)/B(E2)$ is observed at $I = 21\hbar$. The large calculated $B(M1)/B(E2)$ value at $I = 21\hbar$ results from the small $B(E2)$ value. After analyzing the corresponding PRM wave function, we find that, at $I < 20\hbar$, the largest component of the state is $I_s \sim I$ (I_s the angular momentum component along the short axis), while for $I \geq 20\hbar$, the largest one is $I_s \sim I-2$. This leads to the small $B(M1)$ value at $I = 20\hbar$ and small $B(E2)$ values at $I = 20$ and $21\hbar$, and hence a large $B(M1)/B(E2)$ value at $I = 21\hbar$. For D5 and D5-C, their $B(M1)/B(E2)$ values are quite similar and fulfill the characteristics of chiral doublet bands [38,59]. Therefore, they were identified as chiral doublet bands in Ref. [20].

For bands D3 and D4, their $B(M1)/B(E2)$ values are similar. They exhibit a trend that first increases and then decreases with increasing spin. Moreover, their quasi-particle alignments show pronounced similarity over a wide interval of rotational frequency, shown in Ref. [20]. It seems that they are MχD built on identical configuration as in ^{103}Rh [35]. However, as their spectra are interweaved each other at several spins, this possibility is excluded. In the calculations, we use a configuration with three single-j shells to describe D3 and a configuration with four single-j shells to describe D4, shown in Table 1. Admittedly, the present PRM calculations do not agree very well with the data of D3. For D4, the

calculated results reproduce very well the experimental data for $I \geq 19\hbar$.

Note that only the $B(M1)/B(E2)$ ratios for the doublet bands D5 and D5-C have been measured. Hence, the other four pairs of doublet bands are considered only as chiral candidates. As mentioned before, the calculated $B(M1)/B(E2)$ values are similar in the doublet bands. This suggests that the other four candidates might also be chiral doublets. Definitely, further experimental efforts are highly demanded to obtain solid evidence for the chiral doublets interpretation.

The success in reproducing the energy spectra and electromagnetic transition probabilities for the doublet bands in ^{136}Nd motivates us to examine the angular momentum geometries of the observed bands. For this purpose, we calculate the expectation values of the squared angular momentum components along the intermediate (i-), short (s-), and long (l-) axes for the rotor, valence protons, and valence neutrons. Here, the obtained results of bands D2, D5, and D4 are shown in Figs. 4, 5, and 6 as examples, respectively.

As shown in Fig. 4, for both bands D2 and D2-C, the collective core angular momentum mainly aligns along the i-axis at $I \geq 25\hbar$, because it has the largest moment of inertia. It should be mentioned that the s-component of the collective core angular momentum is large and cannot be neglected. Moreover, it exhibits a discontinuous behavior between $I = 19$ and $20\hbar$ in the D2, and between $I = 17$ and $18\hbar$ and $I = 22$ and $23\hbar$ in D2-C. This is understood as the reason of abrupt increases of $B(M1)/B(E2)$ values,
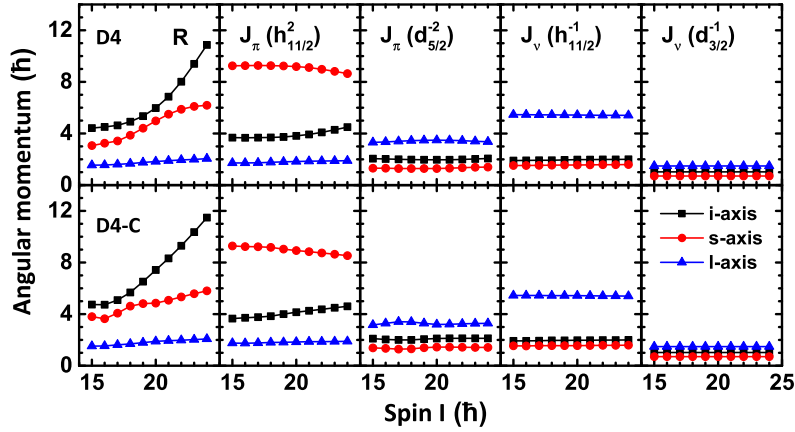
Fig. 6. (Color online.) Same as Fig. 4, but for D4.

as discussed previously. The angular momentum of the three $h_{11/2}$ valence proton particles mainly aligns along the s-axis, and those of valence proton and neutron holes mainly along the l-axis. Such orientations form the chiral geometry of aplanar rotation. But it should be noted that due to the large s-component of the rotor and proton, the total angular momentum lies close to the s–i plane.

For the chiral doublet bands D5 and D5-C, as shown in Fig. 5, the angular momenta have similar orientations at $I \geq 21\hbar$, as those in D2. Namely, the angular momentum of the rotor mainly aligns along the i-axis, the two $h_{11/2}$ valence proton and one $f_{7/2}$ valence neutron particles mainly align along the s-axis, and two $g_{7/2}$ valence proton and one neutron $h_{11/2}$ valence holes mainly along the l-axis. In comparison with those in D2, the s-axis components of the angular momenta of the rotor and $h_{11/2}$ valence proton particles in D5 are about $2\hbar$ smaller. Such orientations form a better chiral geometry of aplanar rotation than that of D2. At $I \leq 21\hbar$, the l-axis components of angular momenta of two $g_{7/2}$ valence proton holes are different in bands D5 and D5-C. For D5, the two proton holes are aligned and contribute $\sim 5\hbar$. However, for D5-C, the alignment happens when the spin increases from $17\hbar$ to $21\hbar$. At $I = 17\hbar$, the two proton holes contribute with $\sim 2\hbar$. At $I = 21\hbar$, the two proton holes contribute $\sim 5\hbar$. Such difference causes the energy difference between the doublet bands in this spin region $\sim 400\,$keV as shown in Fig. 1.

For the bands D4 and D4-C, as shown in Fig. 6, similar aplanar orientation of the angular momenta of the rotor, the particles, and the holes can be observed. This supports that D4 and D4-C are chiral doublets. As discussed previously, there is a band-crossing at $I = 19\hbar$, and the adopted configuration is only suitable for describing the data above band-crossing. One observes that at $I \geq 19\hbar$, the angular momenta of the two $h_{11/2}$ valence proton particles tend to align along i-axis. This leads to the increase of $B(E2)$, and hence to the decrease of $B(M1)/B(E2)$ with the spin as shown in Fig. 3.

In summary, a PRM coupling nucleons in four single-j shells to a triaxial rotor core is developed to investigate the five pairs of nearly degenerate doublet bands recently reported in the even-even nucleus ^{136}Nd. The configurations and corresponding quadrupole deformation parameters (β, γ) are obtained from the constrained CDFT calculations. The experimental energy spectra and available $B(M1)/B(E2)$ values are successfully reproduced. The angular momentum geometries of the valence nucleons and the core support the chiral rotation interpretations not only for the previously reported chiral doublet, but also the other four candidates. Therefore, ^{136}Nd is the first even-even candidate nucleus in which the MχD exists. Five pairs of chiral doublet bands in a single nucleus is also a new record in the study of nuclear chiral-

ity. Further experimental efforts are highly encouraged to obtain solid evidence for MχD interpretations.

References

[1] S. Frauendorf, J. Meng, Nucl. Phys. A 617 (1997) 131.
[2] S.Y. Wang, B. Qi, L. Liu, S.Q. Zhang, H. Hua, X.Q. Li, Y.Y. Chen, L.H. Zhu, J. Meng, S.M. Wyngaardt, et al., Phys. Lett. B 703 (2011) 40.
[3] C. Vaman, D.B. Fossan, T. Koike, K. Starosta, I.Y. Lee, A.O. Macchiavelli, Phys. Rev. Lett. 92 (2004) 032501.
[4] D. Tonev, M.S. Yavahchova, N. Goutev, G. de Angelis, P. Petkov, R.K. Bhowmik, R.P. Singh, S. Muralithar, N. Madhavan, R. Kumar, et al., Phys. Rev. Lett. 112 (2014) 052501.
[5] K. Starosta, T. Koike, C.J. Chiara, D.B. Fossan, D.R. LaFosse, A.A. Hecht, C.W. Beausang, M.A. Caprio, J.R. Cooper, R. Krücken, et al., Phys. Rev. Lett. 86 (2001) 971.
[6] E. Grodner, J. Srebrny, A.A. Pasternak, I. Zalewska, T. Morek, C. Droste, J. Mierzejewski, M. Kowalczyk, J. Kownacki, M. Kisielinski, et al., Phys. Rev. Lett. 97 (2006) 172501.
[7] D.L. Balabanski, M. Danchev, D.J. Hartley, L.L. Riedinger, O. Zeidan, J.-y. Zhang, C.J. Barton, C.W. Beausang, M.A. Caprio, R.F. Casten, et al., Phys. Rev. C 70 (2004) 044305.
[8] S. Zhu, U. Garg, B.K. Nayak, S.S. Ghugre, N.S. Pattabiraman, D.B. Fossan, T. Koike, K. Starosta, C. Vaman, R.V.F. Janssens, et al., Phys. Rev. Lett. 91 (2003) 132501.
[9] S. Mukhopadhyay, D. Almehed, U. Garg, S. Frauendorf, T. Li, P.V.M. Rao, X. Wang, S.S. Ghugre, M.P. Carpenter, S. Gros, et al., Phys. Rev. Lett. 99 (2007) 172501.
[10] C.M. Petrache, Q.B. Chen, S. Guo, A.D. Ayangeakaa, U. Garg, J.T. Matta, B.K. Nayak, D. Patel, J. Meng, M.P. Carpenter, et al., Phys. Rev. C 94 (2016) 064309.
[11] J. Meng, S.Q. Zhang, J. Phys. G, Nucl. Part. Phys. 37 (2010) 064025.
[12] J. Meng, Q.B. Chen, S.Q. Zhang, Int. J. Mod. Phys. E 23 (2014) 1430016.
[13] R.A. Bark, E.O. Lieder, R.M. Lieder, E.A. Lawrie, J.J. Lawrie, S.P. Bvumbi, N.Y. Kheswa, S.S. Ntshangase, T.E. Madiba, P.L. Masiteng, et al., Int. J. Mod. Phys. E 23 (2014) 1461001.
[14] J. Meng, P.W. Zhao, Phys. Scr. 91 (2016) 053008.
[15] A.A. Raduta, Prog. Part. Nucl. Phys. 90 (2016) 241.
[16] K. Starosta, T. Koike, Phys. Scr. 92 (2017) 093002.
[17] S. Frauendorf, Phys. Scr. 93 (2018) 043003.
[18] B.W. Xiong, Y.Y. Wang, arXiv:1804.04437 [nucl-th].
[19] Y.X. Luo, S.J. Zhu, J.H. Hamilton, J.O. Rasmussen, A.V. Ramayya, C. Goodin, K. Li, J.K. Hwang, D. Almehed, S. Frauendorf, et al., Phys. Lett. B 670 (2009) 307.
[20] C.M. Petrache, B.F. Lv, A. Astier, E. Dupont, Y.K. Wang, S.Q. Zhang, P.W. Zhao, Z.X. Ren, J. Meng, P.T. Greenlees, et al., Phys. Rev. C 97 (2018) 041304(R).
[21] J. Meng, J. Peng, S.Q. Zhang, S.-G. Zhou, Phys. Rev. C 73 (2006) 037303.
[22] P.W. Zhao, S.Q. Zhang, J. Peng, H.Z. Liang, P. Ring, J. Meng, Phys. Lett. B 699 (2011) 181.
[23] J. Meng, J. Peng, S.Q. Zhang, P.W. Zhao, Front. Phys. 8 (2013) 55.
[24] P.W. Zhao, Phys. Lett. B 773 (2017) 1.
[25] J. Meng (Ed.), Relativistic Density Functional for Nuclear Structure, International Review of Nuclear Physics, vol. 10, World Scientific, Singapore, 2016.

[26] J. Peng, H. Sagawa, S.Q. Zhang, J.M. Yao, Y. Zhang, J. Meng, Phys. Rev. C 77 (2008) 024309.
[27] J.M. Yao, B. Qi, S.Q. Zhang, J. Peng, S.Y. Wang, J. Meng, Phys. Rev. C 79 (2009) 067302.
[28] J. Li, S.Q. Zhang, J. Meng, Phys. Rev. C 83 (2011) 037301.
[29] J. Li, Phys. Rev. C 97 (2018) 034306.
[30] C. Droste, S.G. Rohozinski, K. Starosta, L. Prochniak, E. Grodner, Eur. Phys. J. A 42 (2009) 79.
[31] Q.B. Chen, J.M. Yao, S.Q. Zhang, B. Qi, Phys. Rev. C 82 (2010) 067302.
[32] I. Hamamoto, Phys. Rev. C 88 (2013) 024327.
[33] H. Zhang, Q.B. Chen, Chin. Phys. C 40 (2016) 024101.
[34] A.D. Ayangeakaa, U. Garg, M.D. Anthony, S. Frauendorf, J.T. Matta, B.K. Nayak, D. Patel, Q.B. Chen, S.Q. Zhang, P.W. Zhao, et al., Phys. Rev. Lett. 110 (2013) 172504.
[35] I. Kuti, Q.B. Chen, J. Timár, D. Sohler, S.Q. Zhang, Z.H. Zhang, P.W. Zhao, J. Meng, K. Starosta, T. Koike, et al., Phys. Rev. Lett. 113 (2014) 032501.
[36] C. Liu, S.Y. Wang, R.A. Bark, S.Q. Zhang, J. Meng, B. Qi, P. Jones, S.M. Wyngaardt, J. Zhao, C. Xu, et al., Phys. Rev. Lett. 116 (2016) 112501.
[37] J. Peng, J. Meng, S.Q. Zhang, Phys. Rev. C 68 (2003) 044324.
[38] T. Koike, K. Starosta, I. Hamamoto, Phys. Rev. Lett. 93 (2004) 172502.
[39] S.Q. Zhang, B. Qi, S.Y. Wang, J. Meng, Phys. Rev. C 75 (2007) 044307.
[40] B. Qi, S.Q. Zhang, J. Meng, S.Y. Wang, S. Frauendorf, Phys. Lett. B 675 (2009) 175.
[41] Q.B. Chen, K. Starosta, T. Koike, Phys. Rev. C 97 (2018), 041303(R).
[42] V.I. Dimitrov, S. Frauendorf, F. Dönau, Phys. Rev. Lett. 84 (2000) 5732.
[43] P. Olbratowski, J. Dobaczewski, J. Dudek, W. Płóciennik, Phys. Rev. Lett. 93 (2004) 052501.
[44] P. Olbratowski, J. Dobaczewski, J. Dudek, Phys. Rev. C 73 (2006) 054308.
[45] D. Almehed, F. Dönau, S. Frauendorf, Phys. Rev. C 83 (2011) 054308.
[46] Q.B. Chen, S.Q. Zhang, P.W. Zhao, R.V. Jolos, J. Meng, Phys. Rev. C 87 (2013) 024314.
[47] Q.B. Chen, S.Q. Zhang, P.W. Zhao, R.V. Jolos, J. Meng, Phys. Rev. C 94 (2016) 044301.
[48] S. Brant, D. Tonev, G. de Angelis, A. Ventura, Phys. Rev. C 78 (2008) 034301.
[49] S. Brant, C.M. Petrache, Phys. Rev. C 79 (2009) 054326.
[50] G.H. Bhat, J.A. Sheikh, R. Palit, Phys. Lett. B 707 (2012) 250.
[51] G.H. Bhat, R.N. Ali, J.A. Sheikh, R. Palit, Nucl. Phys. A 922 (2014) 150.
[52] F.Q. Chen, Q.B. Chen, Y.A. Luo, J. Meng, S.Q. Zhang, Phys. Rev. C 96 (2017) 051303.
[53] M. Shimada, Y. Fujioka, S. Tagami, Y.R. Shimizu, Phys. Rev. C 97 (2018) 024319.
[54] A.A. Raduta, C.M. Raduta, A. Faessler, J. Phys. G, Nucl. Part. Phys. 41 (2014) 035105.
[55] A.A. Raduta, C.M. Raduta, J. Phys. G, Nucl. Part. Phys. 42 (2015) 065105.
[56] A.A. Raduta, A.I.H. Raduta, C.M. Petrache, J. Phys. G, Nucl. Part. Phys. 43 (2016) 095107.
[57] A.A. Raduta, C.M. Raduta, A.I.H. Raduta, J. Phys. G, Nucl. Part. Phys. 44 (2017) 045102.
[58] E.O. Lieder, R.M. Lieder, R.A. Bark, Q.B. Chen, S.Q. Zhang, J. Meng, E.A. Lawrie, J.J. Lawrie, S.P. Bvumbi, N.Y. Kheswa, et al., Phys. Rev. Lett. 112 (2014) 202502.
[59] B. Qi, S.Q. Zhang, S.Y. Wang, J.M. Yao, J. Meng, Phys. Rev. C 79 (2009), 041302(R).
[60] T. Koike, K. Starosta, C.J. Chiara, D.B. Fossan, D.R. LaFosse, Phys. Rev. C 67 (2003) 044319.
[61] S.Y. Wang, S.Q. Zhang, B. Qi, J. Meng, Phys. Rev. C 75 (2007) 024309.
[62] S.Y. Wang, S.Q. Zhang, B. Qi, J. Peng, J.M. Yao, J. Meng, Phys. Rev. C 77 (2008) 034314.
[63] E.A. Lawrie, P.A. Vymers, J.J. Lawrie, C. Vieu, R.A. Bark, R. Lindsay, G.K. Mabala, S.M. Maliage, P.L. Masiteng, S.M. Mullins, et al., Phys. Rev. C 78 (2008) 021305.
[64] E.A. Lawrie, O. Shirinda, Phys. Lett. B 689 (2010) 66.
[65] O. Shirinda, E.A. Lawrie, Eur. Phys. J. A 48 (2012) 118.
[66] B. Qi, S.Q. Zhang, S.Y. Wang, J. Meng, T. Koike, Phys. Rev. C 83 (2011) 034303.
[67] B. Qi, H. Jia, N.B. Zhang, C. Liu, S.Y. Wang, Phys. Rev. C 88 (2013) 027302.
[68] P. Ring, P. Schuck, The Nuclear Many Body Problem, Springer-Verlag, Berlin, 1980.
[69] S.Y. Wang, B. Qi, S.Q. Zhang, Chin. Phys. Lett. 26 (2009) 052102.
[70] J.Y. Zeng, T.S. Cheng, Nucl. Phys. A 405 (1983) 1.
[71] Z. Shi, Z.H. Zhang, Q.B. Chen, S.Q. Zhang, J. Meng, Phys. Rev. C 97 (2018) 034317.